J Mol Model (2001) 7:6–18
DOI 10.1007/s008940100002

ORIGINAL PAPER

**Oscar H. Kapp · Jeanne Siemion · Johnny Kuo
Bradlee A. Johnson · Vidya Shankaran
Richard C. Reba · Jogeshwar Mukherjee**

Comparison of the interaction of dopamine and high affinity positron emission tomography radiotracer fallypride with the dopamine D-2 receptor: a molecular modeling study

Received: 5 May 2000 / Accepted: 9 November 2000 / Published online: 13 March 2001

Abstract We have built a model of the D-2 dopaminergic receptor protein and have docked the agonist dopamine and two dopamine D-2 receptor antagonists, (*S*)-*N*-[(1-allyl-2-pyrrolidinyl)- methyl]-5-(3-fluoropropyl)-2,3-dimethoxybenzamide (fallypride) and (*S*)-*N*-[(1-*iso*-butyl- 2-pyrrolidinyl)methyl]-5-(3-fluoropropyl)-2,3-dimethoxybenzamide (ZYY-106), to its putative active site. We have utilized the structures of bacteriorhodopsin and rhodopsin for modeling the D-2 receptor by homology. Mutation studies and structure-activity studies have been used to refine our model further. Docking exercises of the ligands to the computer-generated D-2 model are used to explain the observed in vitro and in vivo behavior of these compounds. Interactions with the aspartate residue (Asp67) in helix-3 and the serine residues (serine-117 and serine-120) in helix-5 were observed for both dopamine and fallypride. A significant interaction of the phenyl ring of fallypride was observed with Phe121 and Trp155, which was weaker in the case of dopamine. The *N*-allyl group of fallypride is flanked by Phe158 and His162, possibly enhancing π-π interaction and the fluoropropyl group in fallypride is flanked by helix5:Pro124, helix5:phe125 and helix3:Ile75, which seem to form a pocket. These interactions may account for the higher affinity of fallypride for the D-2 receptor compared to dopamine.

O.H. Kapp (✉) · J. Siemion · J. Kuo · B.A. Johnson
V. Shankaran
Enrico Fermi Institute, University of Chicago,
Chicago, Il 60637, USA
e-mail: bud@midway.uchicago.edu
Tel.: +1-773-702-7820, Fax: +1-773-702-9644

R.C. Reba
Department of Radiology, University of Chicago,
Chicago, Il 60637,USA

J. Mukherjee
Department of Medicine/Nuclear Medicine,
Kettering Medical Center, Wright State University,
3535 Southern Boulevard, Dayton, OH 45429, USA

Keywords Dopamine D-2 receptor · Fallypride · Molecular modeling · Ligand docking

Abbreviations *BRD* bacteriorhodopsin · *CG* conjugate gradients · D_{max} maximum derivative · *GPCR* G protein-coupled receptor · *GTP* guanosine triphosphate · *MD* molecular dynamics · *N* nitrogen · *PET* positron emission tomography · *QSAR* quantitative structure activity relationship · *Rho* rhodopsin · *SCR* structurally conserved region · *SD* steepest descent · *SPECT* single photon emission computed tomography · *TM* transmembrane

Introduction

Advances in the understanding of the structural basis of receptor-ligand interaction in the G-protein coupled receptors (GPCR) would aid immensely in the design of new drugs and radiopharmaceuticals and lead to a more rational basis for new drug design. Towards this end, we and others are developing models of GPCRs and are docking various molecules for post-synaptic receptors that will enhance the study of the role of the receptors. [1, 2, 3, 4, 5, 6, 7, 8, 9, 10, 11, 12, 13, 14, 15, 16, 17, 18, 19, 20, 21, 22, 23, 24, and references cited within]

The dopaminergic neurotransmitter receptor system has been related to human brain disorders such as schizophrenia, tardive dyskinesia, dystonia, Parkinson's disease, Huntington's disease, substance abuse and alcoholism. Five post-synaptic dopamine receptor subtypes have been identified.[25] Gene organization based on the presence or absence of introns in the protein-coding region has differentiated two subfamilies, the D-1 like (without introns) consisting of D-1 and D-5 and D-2 like (with introns) consisting of D-2, D-3 and D-4. We have been involved in the development of radiopharmaceuticals that may be suitable for the in vivo study of D-2 receptors. One such agent, fallypride ((*S*)-*N*-[(1-allyl-2-pyrrolidinyl)- methyl]-5-(3-fluoropropyl)-2,3-

dimethoxybenzamide) has been well characterized in terms of its in vitro pharmacology and its radiotracer analog, [^{18}F]fallypride, has been used in vivo in order to study the distribution of the receptors.[26, 27, 28] Understanding the molecular interactions of fallypride with the tertiary structure of the receptor would be useful in order to enhance selectivity as well as gain insights on the design of a D-3 or a D-4 receptor-subtype selective ligand.

Using protein modeling methods in order to obtain three-dimensional structures of GPCRs, such as described by Ballesteros and Weinstein,[29] several investigators have recently modeled the dopamine D-2 receptor.[18, 20, 30, 31, 32, 33] Molecular modeling methods have the potential to refine structures of the radioligands in order to meet the criteria for use in positron emission tomographic (PET) studies. We report here the development of a dopamine D-2 receptor molecular model and investigate its interaction with the agonist dopamine, and two antagonists, (*S*)-*N*-[(1-allyl-2-pyrrolidinyl)methyl]-5- (3-fluoropropyl)-2,3- dimethoxybenzamide (fallypride) and (*S*)-*N*-[(1-*iso*-butyl-2- pyrrolidinyl)methyl]-5-(3-fluoropropyl)-2,3-dimethoxybenzamide (ZYY-106).

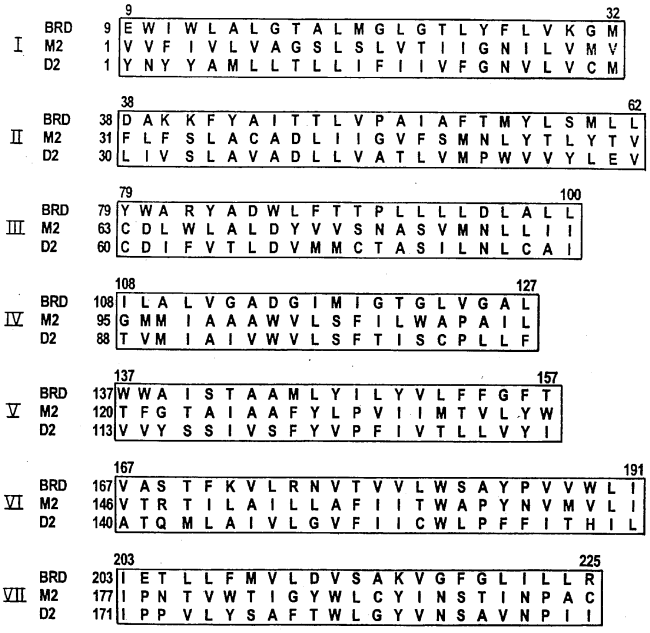

Fig. 1 Alignment of D2 with the bacteriorhodopsin sequence. The muscarinic sequence m2 is shown for comparison. The helix numbers are indicated on the *left* in roman numerals. The numbering of the three sequences is indicated on the *left* of each transmembrane region which is enclosed in a box

Methods

Our method of modeling the GPCRs is based on homology modeling using bacteriorhodopsin (BRD) coordinates followed by refinement based on current supporting data (mutation, binding, protein modeling). The coordinates of the BRD structure used to model our receptors are based on a low resolution electron microscope result.[34] The resolution in X and Y is 3.5 Å while in Z it is only about 10 Å. Thus, only approximate comparisons can be made, and in fact, the low resolution in Z causes sufficient uncertainty that the positions of the individual amino acids along the seven transmembrane domains are somewhat ambiguous. Thus, our approach is to generate several hypothetical receptors differing in such parameters as the choice of registration of the transmembrane domains. The software we chose for this task is the suite of programs Insight, Discover and Homology, by MSI, Inc. The homology module is based on the work of Greer.[35] Using this software, described in detail below, we identify structurally conserved regions (SCRs) and constrain the system by limiting the motion of these segments of the sequence during the modeling process. A number of groups have developed theoretical models of GPCRs. We have used a combination of several different approaches.

We have devised a computational method to assist traditional methods in the development of selective ligands as potential radiopharmaceuticals for GPCRs. Our method is divided into the following main steps: 1. Modeling Receptors (Receptor backbones; Detailed modeling procedure, and Structure refinement), 2. Energy minimized small molecules and in-vitro affinities, 3. Docking studies of ligands with models, 4. Assessment of interactions (structure of active-site and quantitative analysis of interaction).

Modeling receptors

The steps in modeling the receptor are summarized below followed by detailed comments of each step.

1. Edit sequence file to remove loops and replace with 5 glycine residues.
2. Align D-2 sequence with BRD based on published consensus alignment.
3. Transfer coordinates from BRD to D-2.
4. Generate (de novo) loop coordinates.
5. Assign coordinates to amino and carboxyl terminal.
6. Energy minimize splices.
7. Optimize sidechain conformations.
8. Energy minimize sections of helix.
9. Adjust ϕ/ψ angles of α-helix for Pro distortion.
10. Test model for agreement with mutation data by docking of dopamine.
11. Adjust rotation and relative orientation of helices to account for mutagenesis data.
12. Relax receptor/ligand complex.
13. Run molecular dynamics on complex.

Detailed modeling procedure

We used the commercial software available from MSI, Inc. (Insight, Discover and Homology) to build several models of the D-2 (dopaminergic) receptor using the amino acid sequence of human D-2 obtained from the PIR.

- **Step 1.** We replaced the loop regions (for which there are no available coordinates) with five glycine residues (per loop) to simplify the computation. We are interested in the ligand/receptor interaction area that occurs in the transmembrane region.
- **Step 2.** We used an alignment of D-2 with BRD based on published consesus alignments (Fig. 1) [23, 33] to obtain the coordinates of the backbone and side chains of the seven transmembrane regions. This involves *a*. superfamily alignment – based on conserved residues; *b*. functional similarities between BR and rhodopsin – retinal binding site at Lys; *c*. mutation data on/and conservation of binding pocket residues; *d*. helical wheel and e. hydrophobicity plots.
  Dopamine receptors are part of the G-protein coupled receptor (GPCR) family and sequence alignment of the GPCRs has been studied by several groups and is well established and agreed upon. [18, 20, 30, 31, 32, 33] Two methods were used in the superfamily alignment. The first is manual alignment re-

lying on invariant residues. Within the superfamily there is about 30% homology and within a subfamily the homology rises to >75%. The second method of alignment uses the Needleman and Wunsch algorithm [36, 37] for amino acids.

Although their sequence homology is quite low (10%), there are many reasons supporting the use of bacteriorhodopsin coordinates to model GPCRs. Henderson and Schertler [34] discussed the structural similarity between BRD and Rho, a member of the GPCR family. They have measured crystallographic projection structures of BRD and Rho showing that both proteins consist of seven transmembrane helices with an extracellular amino terminus. [34, 38] BRD and Rho both bind retinal, a light activated chromophore, with a primary binding site at a lysine residue in the seventh helix.

Hydrophobicity plots also suggest that GPCRs consist of seven transmembrane regions (TMR). The exact alignment of BRD with D-2 was determined by accounting for 1. amphipathicity in the helical wheel projections; 2. conservation of binding pocket residues; 3. mutation data; [18] and 4. functional similarities (e.g., retinal binding site) between BRD and Rho. Table 1 provides a comparison of the numbering of the transmembrane domains used in this paper as well as that of published work. It is often difficult to compare results because of the lack of uniformity in the numbering system used. This table may be used as a quick reference for comparison of various author's work.

- **Step 3.** After the sequence alignment is complete, the reference (BRD) coordinates are transferred to the model. First the BRD coordinates are transformed into the same coordinate frame as the model. The backbone and conserved sidechain coordinates are transferred directly. Where the sidechains differ, the dihedral angles in common are aligned. The more distal atoms of the replacement residue are given an extended conformation. New charges and potential function types are taken from the residue library.
- **Step 4.** De novo coordinates for the variable region of the model protein were generated using the random tweak method of Levinthal. [39] Different conformations are generated using geometric constraints to produce a group of loop structures which are near the energy minimum.
- **Step 5.** The *N*- and *C*-terminal ends of the protein are assigned coordinates from the standard amino acid library.
- **Step 6.** The splice points between the TMR, loops and terminal regions may have long, short or *cis* peptide bonds. These are repaired by doing a local energy minimization with optional torsion forcing of the peptide bonds to 180 degrees. Energy minimizations are carried out using the consistent valence force-field (CVFF), a generalized valence force-field. [40] Twenty atom types are defined by the Molecular Simulation Inc. software with each line defining a new potential function atom type name, giving its atomic mass, element, and a description of the atom type. The Discover program uses the atom types to assign parameters from the force-field file.
- **Step 7.** Side chain conformations are optimized to eliminate bumping and minimize energy. The rotamer library of Ponder and Richards [41] is used. The algorithm suggested by Mas et al. [42] is used to determine the best combination of conformations. In this method a list of moving residues is specified. The lowest energy rotamer is selected for the first residue, then the second residue, and so on. A cycle is defined as one complete pass through the list. The search stops when the energy does not change appreciably from one cycle to the next.
- **Step 8.** The entire model is geometrically optimized with Discover by energy minimizing subsets of the model. Portions (e.g., terminal residues. loops, mutated side chains, all side chains) of the model were relaxed while the rest remained fixed. The backbone was not relaxed in order to maintain a model structure close to the reference BRD.
- **Step 9.** We adjusted for proline distortion of the ϕ, ψ angles of the model α-helix using template helices. BRD helix 2 and BRD helix 4 served as templates for α-helices with and without, respectively, a proline induced bend. Energy minimization with template forcing was used to remove or add a bend in the model α-helix. D-2:helix3 had a kink smoothed out at threonine72 residue. D-2:helix4:proline104 and D-2:helix5:proline124 had a bend added. Proline bends were shifted in D-2:helix2:alanine42 to D-2:helix2:proline47 and D-2:helix6:phenylalanine159 to D-2:helix6:proline157. Prolines near the end of the TMR (e.g., D-2:helix7:proline172, 173, 191) were not adjusted.
- **Step 10.** The validity of the D-2 receptor model was tested by docking its natural agonist, dopamine, in the putative binding site. We compare the model active site residues with those obtained from mutational alteration experiments. Table 2 provides a compilation of mutational studies found in the literature. The receptor/ligand model was energy minimized with distance constraints applied at the dopamine nitrogen-aspartate67 salt bridge, and serine 117 and 120 hydrogen bonding sites followed by minimization without constraints. Examination of the resulting complex showed appropriate bonding distances and freedom from bumping (close contacts).
- **Step 11.** Where necessary, helices are rotated, tilted, and/or shifted to bring amino acids suspected of being important to

Table 1 Correlation of the various residue numbering schemes used by authors whose molecular models are referred to in this paper

Helix	Residue	This work	Teeter	Kallmeyer	Baldwin
1	MET	24			I23
2	LEU	30			II6
2	ASP	38		207	
2	ALA	42			II18
2	PRO	47			II23
2	TRP	48	56		II24
2	VAL	54			II30
3	CYS	60			0
3	PHE	63	82	307	III3
3	ASP	67	86	311	III7
3	MET	70	89		III10
3	CYS	71	90	315	III11
3	THR	72			III12
3	ILE	81			III21
4	THR	88			IV4
4	TRP	95	115	403	IV11
4	SER	98	118	406	IV14
4	ILE	101			IV17
4	SER	102	122	410	IV18
4	PRO	104			IV20
4	PHE	107			IV23
5	VAL	113			V3
5	SER	117	141	505	V7
5	SER	120	144	508	V10
5	PHE	121	145	509	V11
5	TYR	122		510	
5	PRO	124		512	V14
5	ILE	133			V23
6	ALA	140			VI1
6	PHE	151		609	
6	TRP	155	182	613	VI16
6	PRO	157			VI18
6	PHE	158	185	616	VI19
6	PHE	159	186	617	VI20
6	LYS	164			VI25
7	ILE	171			VII –2
7	PRO	173			VII0
7	TYR	176	208	707	VII3
7	THR	180	212		VII7
715	TYR	184	216	715	VII11
7	PRO	191			VII18
7	ILE	193			VII20

Table 2 Compilation of mutation data gathered from the literature.

Baldwin Notation	Mutation		Receptor	Binding Effect	Reference
	Ref. Notation	Our Notation[a]			
II	D46	D38	D_2 α β D_1	Important agonist binding, allosteric regulation, increased K_d for agonist	Probst et al. [33], Neve et al. [46] Horstman et al. [5] Dohlman et al. [60] Tomic et al. [19]
II: 14	D79A D79 N	D38	Beta-2: hamster Beta-2: man		Strader et al. [10, 11] Chung et al. [61]
III	D86	D67	D_1 D_2 Rho		Tomic et al. [19] Mansour et al. [45], Strange et al. [14] Probst et al. [33]
III	C89A		D_1	Decreased affinity	Tomic et al. [19]
III	M89	M70	D_2		Strange et al. [14]
III	D	D70	5HT, D, Adren.		Strader et al. [13]
III: 0	C106		Beta-2: hamster		Dixon et al. [62]
III:7	D113 N		Beta-2: hamster		Strader et al. [10]
V	S141	S117	D_1		Tomic et al. [19]
V	S144A	S120A	D_2		Mansour et al. [45]
V	F145A S198A	F121A S116	D_2 D_1: man	Increased K_d	Strange et al. [14] Pollock et al. [8]
V: 7	S204A S199A	S117	Beta-2: man D_1: man		Strader et al. [12] Pollock et al. [8]
V: 10	S207A S204A S242A S202A	S120	Beta-2: man Alpha-2a: man 5HT2: man D_1: man		Strader et al. [12] Wang et al. [23] Kao et al. [63] Pollock et al. [8]
VI	C181S	C154S	β	Structural	Fraser et al. [64]
VI	T168	Loop 6–7	α	Constitutive activation	Kjelsberg et al. [65]
VI	F186A	F159A	D_2 M	No affinity	Trump-Kallmeyer et al. [20], Choudhary et al. [66], Summers et al. [15] Probst et al. [33]
VI	H189	H162	D_{234}	Bind, antagonist affinity	Livingstone et al. [30, 31]
VI	W182 F412 N N385 V T355 N	W155	M3 Rho Alpha-2a: manq 5HT1A: man 5HT1B: man	Decreased affinity binding rhodopsin	Wess et al. [24], Nakayama et al. [67] Suryanarayana et al. [17] Guan et al. [68] Oksenberg et al. [69]
VII: 13	N318 K N218 N385	N186 Y186	Beta-2: hamster 5HT	 Antagonist binding	Strader et al. [10] Summers et al. [15] Guan et al. [68]
VII: 14	S319A S219	S187	Beta-2: man		Strader et al. [12] Summers et al. [15]
VII	N222A	N190A	5HT	No agonist affinity	Chanda et al. [70]
VII	T212	T180	D_{234}	Important to high affinity	Guan et al. [68], Oksenberg et al. [69], Suryanarayana et al. [17]
VII	W216Y	Y184 [D_2]	D_1	Decreased antagonist affinity, no change agon. affinity	Tomic et al. [19]

[a] Our notation refers to our residue numbers in the D2 models. This table expands on the results of an earlier table of Baldwin (1993).

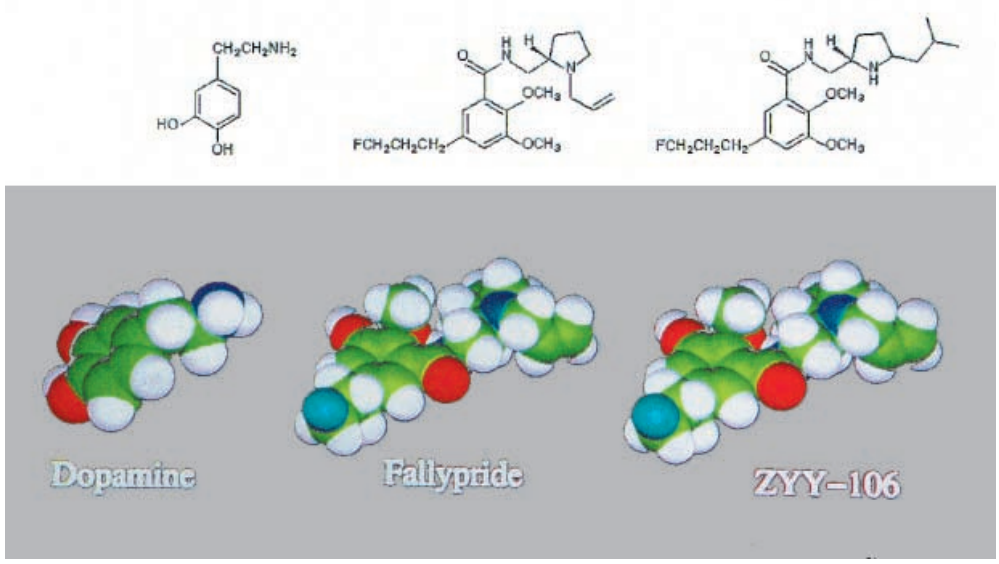

Fig. 2 Chemical structures of *top:* dopamine, fallypride, ZYY-106, *bottom:* spaced-filled models of the above

binding (based on mutational studies) into the vicinity of the active binding pocket. Structural refinement is also accomplished by following Baldwin's model for GPCR based on the Rho projection map and statistical analysis of residue characteristics.[43, 44]

- **Step 12.** Relax receptor/ligand complex using distance contraints followed by removal of constraints.
- **Step 13.** Run molecular dynamics on complex. Further comments on this step can be found in the following sections.

Molecular models of dopamine and fallypride

The ligands for docking (Fig. 2), dopamine, fallypride and ZYY-106, were energy minimized using the method of conjugate gradients. The Molecular Simulations version of this algorithm includes bond stretching, angle bending, torsion deformation, van der Waals interactions, out-of-plane bending and electrostatic interactions.

Docking experiments of ligands with the receptor models

In the initial docking exercises distance constraint minimization was carried out using Steepest Descent to a maximum derivative of about 1.0. Receptor ligand models were checked for bumping. In further docking studies the distance constraints are removed and molecular dynamics performed.

Minimization was first carried out with Steepest Descent to D_{max} <10 and then with Conjugate Gradient to D_{max} <0.1. The backbone of the helices was always kept fixed to maintain the relative helical orientation. These backbone constraints are removed during the next stage of molecular dynamics. For the receptor and complex minimization the CVFF (consistent valence force-field) was used with a dielectric of 4, a nonbond cutoff of 8.00 Å, a cutoff distance of 7.000 Å and a switching distance of 1.5. The nonbond cutoff is the point at which nonbond interactions are neglected for pairs of atoms separated by a distance greater than the cutoff value. The switching distance is the distance over which the switching function is applied. The cutoff distance is the point at which bonding interaction is cut off. Cross terms were included and the Morse potential utilized for the bond-stretching term.

Before beginning MD, the backbone of the interaction region or binding pocket was tethered, and the backbone outside of the interaction region was held fixed. We use the term "interactive region" or "binding pocket" to describe the entire interior pocket of the receptor and the term "active site" to refer to residues immediately surrounding the ligand. The sidechains were allowed to rotate freely, and MD was run on the complex to allow the ligand and sidechains to explore conformational space. We used the Verlet [22] leapfrog algorithm to integrate the equations of motion with a timestep of 1 femtosecond. This timestep was our choice based on a consideration of the tradeoff between accuracy and computational efficiency. MD was done under constant volume and temperature (NVT ensemble). The temperature was 310 K (37 C). The NVT ensemble was chosen because it is appropriate for conformational searches of molecules in vacuum without periodic boundary conditions. Typical MD used 5000 steps to equilibrate and 50,000 steps of simulation. At the end of the MD, the history file was analyzed to determine the lowest energy conformation generated during the dynamics.

This conformation was then minimized with Steepest Descent to D_{max} <10 and Conjugate Gradient to D_{max} <0.1. The distance constraints were released, and then the complex was minimized again with Conjugate Gradient to D_{max} <0.1 to obtain the docked structure. Finally, we explored different initial docking configurations and repeated the steps described above.

Assessment of interactions

For the subclass of receptors that bind cationic amines, there is a conserved aspartate in the third transmembrane domain (helix3:Asp67) that forms electrostatic interactions with the ammonium part of the ligand. [45, 46] For all our initial docking calculations, a distance constraint was set to hold the ammonium nitrogen within 2.9 Å of the Asp67 oxygens. While the N head was constrained to be close to the Asp, the ligand tail was positioned to reduce bumping with the receptor interior. Consideration was given to possible H-bonding, hydrophobic interaction sites between receptor sidechains and ligand tail groups. We reviewed current published models and mutagenesis data. The interaction region was defined to include residues within 12 Å of the ammonium N (which was fixed 2.9 Å from the Asp). The backbone of the receptor in the interaction region was tethered. The backbone of the receptor outside the interaction region was held fixed during MD. All sidechains and ligands were allowed to move.

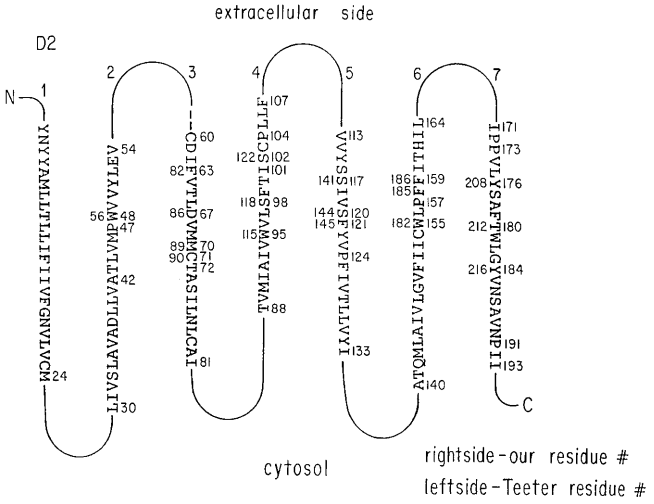

Fig. 3 Schematic of the seven transmembrane domains of the D2 receptor. The vertical positioning of each helix corresponds to its approximate position (Z axis) in the membrane. The sequence number of the residues of the D2 receptor using our numbering system is shown on the *right side* while that of Teeter et al. [18] is shown on the *left*

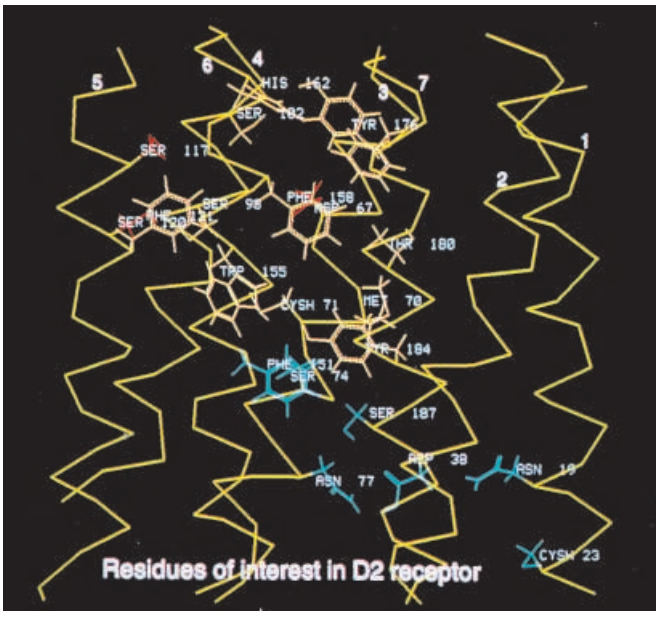

Fig. 4 Side view of the complete model structure of the D2 receptor showing amino acids with possible functional roles. The α-helical backbone of the transmembrane regions are shown in *yellow* and are numbered 1–7. The residues that Teeter *et al.* [18] suggests are involved in the functioning of the Na^+ channel are shown in *blue*. Ser117 and 120 on helix 5 and Asp67 on helix 3 are shown in *red*

Results

Receptor model

Table 1 correlates the various residue numbering schemes used by authors to whose models we refer. Our numbering scheme which is continuous from the amino to the carboxyl terminals was determined by the MSI software package we used during the homology modeling stage. Our residue numbers differ from the PDB because we replaced the variable length loop regions with segments of five glycines for simplification. Teeter et al. [18] used a numbering scheme that was continuous throughout the entire sequence. Trumpp-Kallmeyer et al., [20] and Baldwin [43] used continuous sequence numbering within each TM helix, prefacing the residue number with the helix number (1–7 or I-VII).

Figure 1 shows the sequence alignment of the structurally conserved regions (SCRs) of D-2 with those of BRD. The SCRs define the regions where the actual coordinate data were transferred from BRD to D-2. The GPCR human m2 (muscarinic) sequence is shown for comparison. [6] The seven α-helices are labeled on the left in Roman numerals. The sequence numbers refer to the SCRs; the loops and terminal regions have been omitted. The BRD sequence numbering is 9–255 (from PDB), D-2 is 1–193 (from MSI software), m2 is 1–200. The m2 and D-2 numbering differ from each other because of their different loop structure.

Figure 2 shows the chemical structures of **top**: dopamine, fallypride and. ZYY-106, and **bottom**: space-filled models of these molecules.

Figure 3 shows a schematic of the seven transmembrane (α-helical) domains of the D-2 receptor. The loop

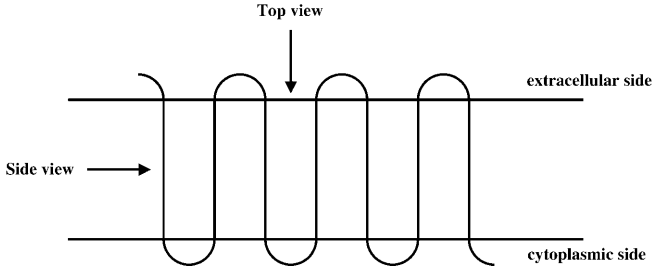

Scheme 1 In the figure captions the expression "top-view" refers to the view of the receptor looking from the extracellular side through the membrane towards the cytosol. In this view the helical shape of most of the transmembrane domains is seen end-on. The expression "side-view" refers to the view of the receptor along the plane of the membrane with the extracellular side of the receptor oriented to the top of the figure

regions are represented by a short curved line. The extracellular side is to the left. The vertical positioning of each helix corresponds to its approximate relative position (Z axis) in the membrane. The sequence number of the residues of the D-2 receptor using our numbering system is shown on the right side while that of Teeter et al., [18] is shown on the left.

Figure 4 shows a side view (for explanation see scheme 1) of the complete model structure of the D-2 receptor showing amino acids with possible functional roles. The α-helical backbone of the transmembrane regions are shown in yellow and are numbered 1–7. The residues that Teeter et al., [18] suggests are involved in

the functioning of the Na^+ channel are shown in blue. Ser117 and 120 on transmembrane helix 5 and Asp67 on helix 3 are shown in red.

Figure 5 shows the helical wheel for BRD and our model of D-2 GPCR analogous to Baldwins figure five [43]. The helical backbone is colored green and the beta carbons are colored according to the Engelman and Steitz [47] hydrophobic scale.

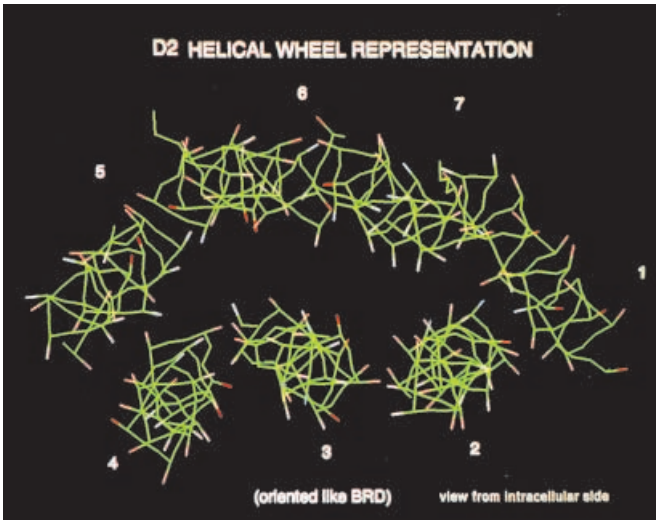

Fig. 5 The helical wheel representation of D2 dopaminergic receptor. The view is from the intracellular side. The backbone is colored *green* and the beta carbons are colored by the hydrophobicity scale of Engelman and Steitz [47] where *purple/blue* is hydrophilic (K, R, E, D), *lavender* is N, *white* is P, Y, *light pink* is T, S, *dusty rose* is W, A, and *red/orange* is lipophilic (I, V, L, F, M). This figure illustrates the relative difference in helical orientation of BRD and our model of D2 (a GPCR)

Docking ligands to the D2 receptor model

Figure 6 shows top views of the model of the D-2 receptor docked with dopamine (left) and fallypride (right). The binding of both ligands occurs in the same relative location within the helices.

Figure 7 (side view) shows details of the docking of dopamine with the D-2 receptor model. The α-helical backbone of the transmembrane regions are shown in yellow. The figure shows details of the docking where the catecholic hydroxyls are shown to interact with the serine residues 117 and 120 on helix 5 (highlighted in red on right side of figure). Dopamine was docked in the D-2 receptor by constraining the ammonium nitrogen to the oxygens in helix3:Asp67 (highlighted in red on left side of figure) to form a salt bridge and by constraining the H's of the catechol hydroxyl groups to the oxygens of helix5:Ser117,120 to form hydrogen bonds. Mutagenesis data support the primary binding sites at helix3:Asp67 and helix5:Ser117,120. Distance monitors, indicated in white, show interaction distances of 3.80 and 3.23 Å between the hydroxyl moieties of dopamine and Ser117 and Ser120. The nitrogen of dopamine is shown to interact with Asp67 with a distance of 3.67 Å. Other aromatic residues (colored orange) in the binding pocket region surround dopamine (Phe121 and orthogonally, Trp155).

Figure 8 (side view) and Fig. 9 (top view) show details of the docking of fallypride with the D-2 receptor model. The α-helical backbone of the transmembrane regions are shown in yellow. Asp67 (helix 3) and Ser117,120 (helix 5) are colored red; other residues of interest are colored orange. In this experiment, fallypride was docked by constraining the ammonium nitrogen to the oxygens in Asp67 (highlighted in red on left side of figure) to form a salt bridge and by constraining the me-

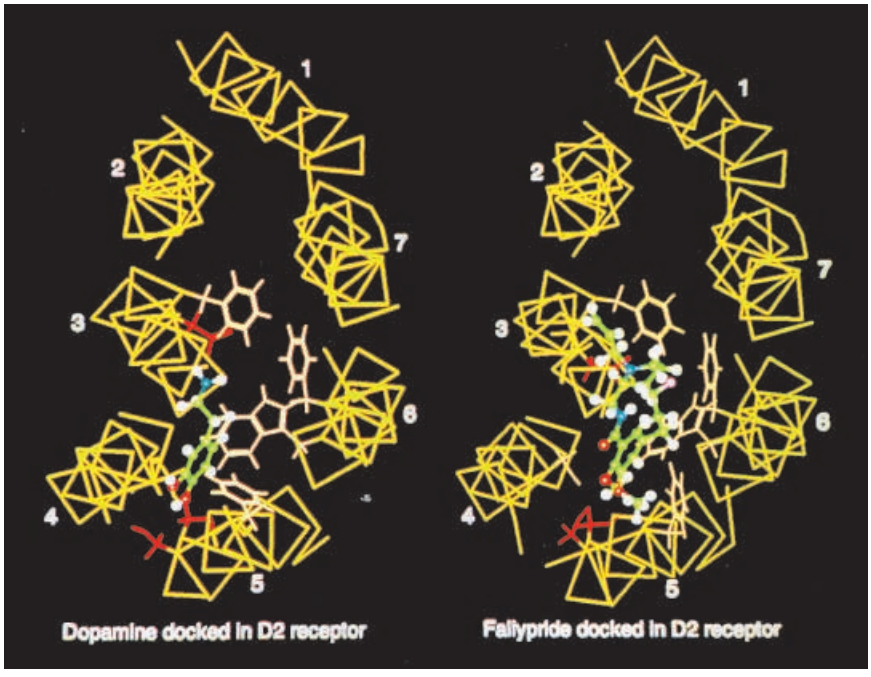

Fig. 6 Top views of the model of the D2 receptor docked with dopamine (*left*) and fallypride (*right*). The α-helical backbone of the transmembrane regions are shown in *yellow*. The binding of both ligands occurs in the same relative location within the helices

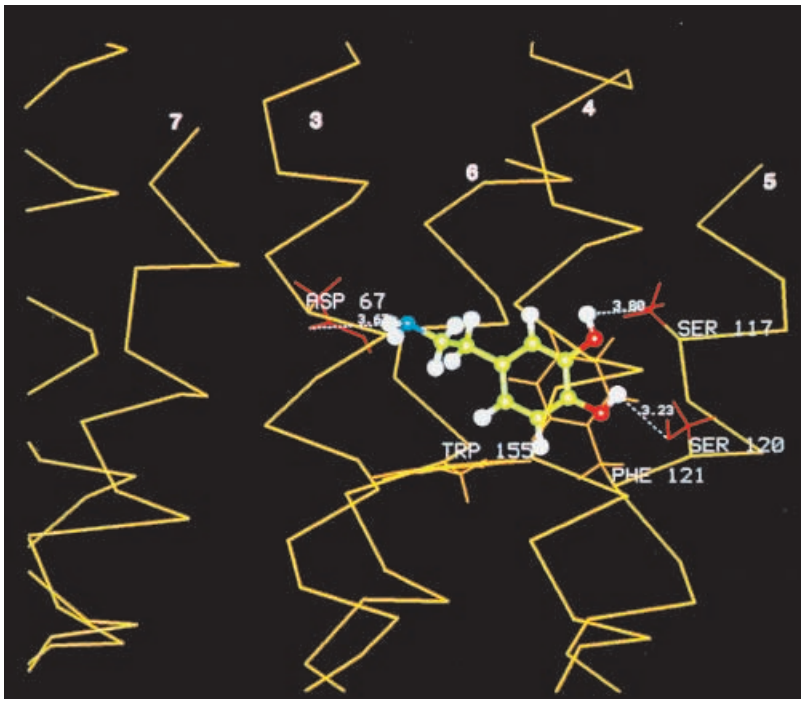

Fig. 7 Detail of side view of docking of dopamine with the D2 receptor model. The α-helical backbone of the transmembrane regions are shown in *yellow*. Helix3:Asp67 and helix5:Ser117,120 are colored *red*; other residues of interest are colored *orange*. Distance monitors, indicated in *white*, show interaction distances of 3.80 and 3.23 Å between the hydroxyl groups of dopamine and Ser117 and 120, respectively. The nitrogen of dopamine is shown to interact with Asp67 with a distance of 3.67 Å (distance monitor partially obscured). Other aromatic residues (colored *orange*) in the binding pocket surround dopamine (Phe121 and Trp155). The extracellular side of the membrane is at the top of the figure

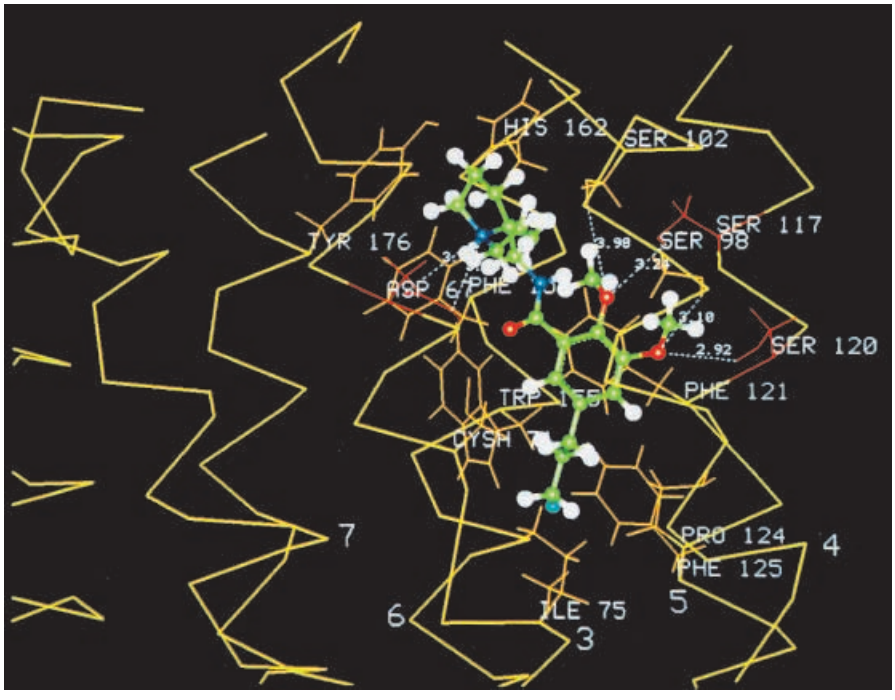

Fig. 8 Detail of side view of docking of fallypride to the D2 receptor model. The α-helical backbone of the transmembrane regions are shown in *yellow*. Asp67 and Ser117,120 are colored *red*; other residues of interest are colored *orange*. Distance monitors, indicated in *white*, show the methoxy oxygens of fallypride interacting with Ser117 and Ser120 at distances of 3.24 and 2.92 Å, respectively. Ser98 and Ser102 on helix 4 are also shown to interact with the methoxy oxygens with distances of 3.10 and 3.98 Å, respectively. The nitrogen of fallypride is shown to interact with two oxygens of Asp67 with distances of 3.71 and 3.23 Å (partially obscured from view). In addition, the Cys71 (Helix3) is shown to interact with the carbonyl oxygen of fallypride with a distance of 2.49 Å (not shown). Several aromatic and hydrophobic residues in the binding pocket surround fallypride (Ile75, Phe121, Pro124, Phe125, Trp155, Phe158, His162, and Tyr176)

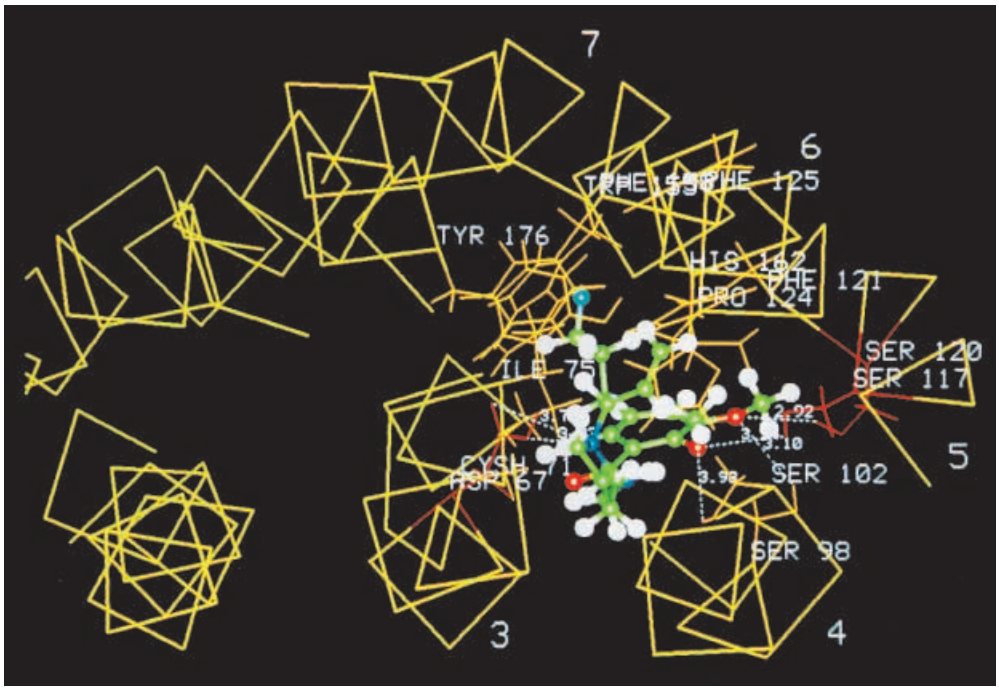

Fig. 9 Detail of top view of docking of fallypride to the D2 receptor model. The α-helical backbone of the transmembrane regions are shown in *yellow*. Asp67 and Ser117,120 are colored *red*; other residues of interest are colored *orange*. The figure shows a detail of the top-view of the docking where the methoxy groups are shown to interact with serines 98, 102, 117, 120 (seen on the *right side* of the figure)

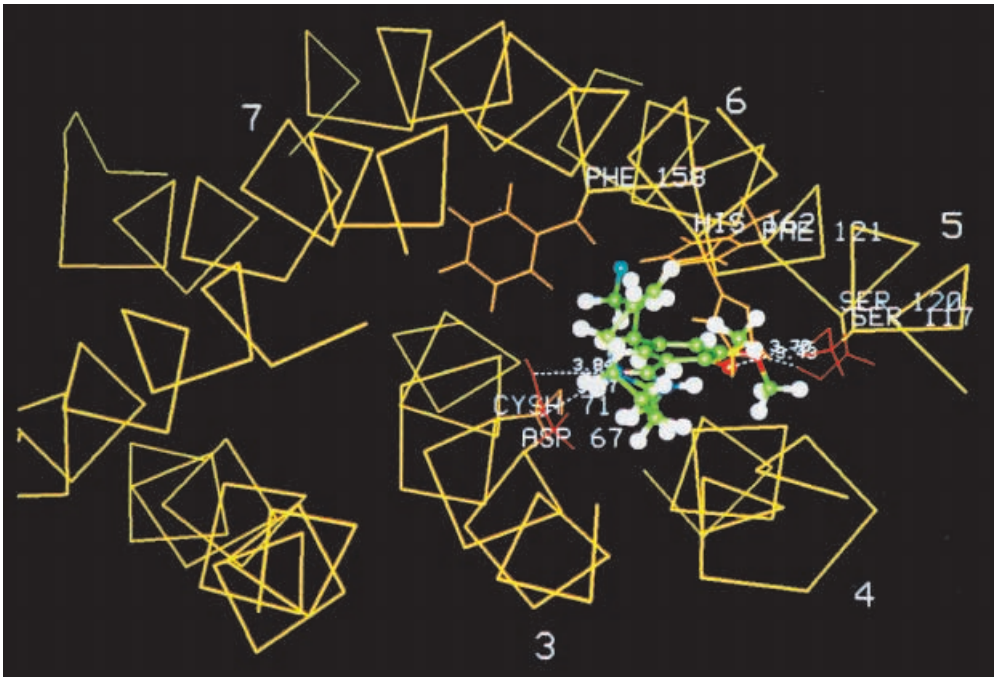

Fig. 10 Detail of top view of fallypride docked to the D2 receptor model without the distance constraints to Ser117,120. The α-helical backbone of the transmembrane regions are shown in *yellow*. Asp67 and Ser117120 are colored *red*; Cys71, Phe121, Phe158, and His162 are colored *orange*. Distance monitors, colored *white*, show interaction distances of 3.70 and 3.43 Å between the methoxy oxygens of fallypride and Ser117,120. The nitrogen of fallypride is shown to interact with the two oxygens of Asp67 with distances of 3.37 and 3.84 Å. Phe121 appears coplanar with the benzamide ring of fallypride, and Phe158 and His162 form a pocket flanking the *N*-allyl moiety of fallypride

thoxy oxygens to the H's of Ser117,120 to form hydrogen bonds. Distance monitors, indicated in white, show interactions distances of 3.24 and 2.92 Å between the methoxy oxygens of fallypride and Ser117 and Ser120. Ser98 and Ser102 on helix 4 are shown to interact with methoxy oxygens of fallypride with distances of 3.10 and 3.98 Å. In addition, Cys71 is shown to interact with the carbonyl oxygen with a distance of 2.49 Å. The nitrogen of fallypride is shown to interact with Asp67 oxygens with distances of 3.23 and 3.71 Å.

Other aromatic and hydrophobic residues in the binding pocket surround fallypride. Helix5:Phe121 appears coplanar with the benzamide ring of fallypride, and helix6:Trp155 is located in close proximity to the benzamide ring. Helix7:Tyr176 appears near the pyrrole ring. The Phe158 and His162 (helix 6) flank the *N*-allyl moiety. Lastly, Helix5:Pro124, Helix5:Phe125, and Helix3:Ile75 form a pocket surrounding the fluoropropyl group of fallypride.

Figure 10 shows the top view of a second docking of fallypride to the D2 receptor model in which the distance

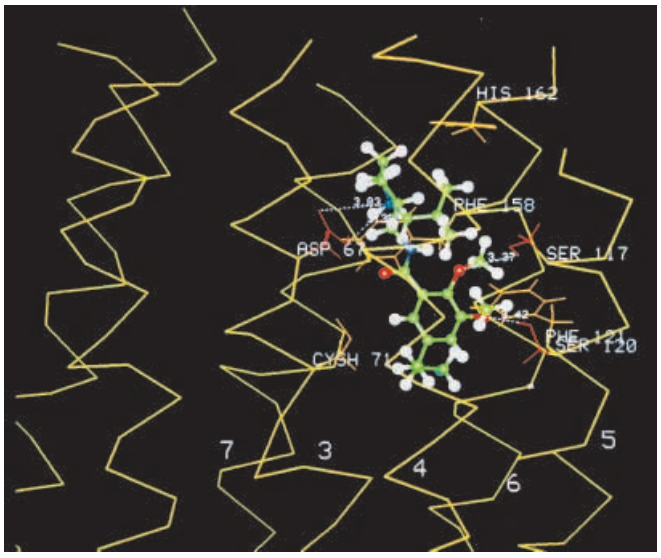

Fig. 11 Detail of side view of ZYY-106 docked to the D2 receptor model without distance constraints to Ser117,120. The α-helical backbone of the transmembrane regions are shown in *yellow*. Asp67 and Ser117,120 are colored *red*; Cys71, Phe121, Phe158, and His162 are colored *orange*. Distance monitors, colored *white*, show interaction distances of 3.37 and 3.42 Å between the methoxy oxygens of fallypride and Ser117,120. The nitrogen of fallypride is shown to interact with the two oxygens of Asp67 with distances of 3.39 and 3.83 Å. Although Phe158 and His162 still flank the *N*-iso-butyl moiety of fallypride, steric interactions between the bulky iso-butyl group and these residues pushes the ligand slightly deeper into the binding pocket and effectively prevent base stacking between the benzamide ring and Phe121

constraints between the methoxy moieties and Ser117,120 were released. The α-helical backbone of the transmembrane regions are shown in yellow. Asp67 and Ser117,120 are colored red; Cys71, Phe121, Phe158, and His162 are colored orange. Distance monitors, colored white, show interaction distances of 3.70 and 3.43 Å between the methoxy oxygens of fallypride and Ser117,120. The nitrogen of fallypride is shown to interact with the two oxygens of Asp67 with distances of 3.37 and 3.84 Å. Phe121 appears coplanar with the benzamide ring of fallypride, and Phe158 and His162 form a pocket flanking the *N*-allyl moiety of fallypride. In contrast to the docking of fallypride with distance constraints to the Ser117,120 residues, docking fallypride without these distance constaints did not bring Cys71 in close enough proximity to the carbonyl oxygen of fallypride for any potential hydrogen bonding interactions to occur.

Figure 11 shows the side view of the docking of ZYY-106 to the D2 receptor model. The α-helical backbone of the transmembrane regions are shown in yellow. Asp67 and Ser117,120 are colored red; Cys71, Phe121, Phe158, and His162 are colored orange. The ZYY-106 ligand was docked to the D2 receptor model by constraining the ammonium nitrogen to the oxygens of Asp67; as with the second docking of fallypride, no distance constraints between the ligand and Ser117,120 were used. Distance monitors, colored white, show interaction distances of 3.37 and 3.42 Å between the methoxy oxygens of ZYY-106 and Ser117,120. The nitrogen of ZYY-106 interacts with the two oxygens of Asp67 with distances of 3.39 and 3.83 Å. Although Phe158 and His162 still flank the *N-iso*-butyl moiety of ZYY-106, steric hindrance between the bulky iso-butyl group and these residues pushes the ligand slightly deeper into the binding pocket. As a consequence of the ligand being shifted slightly deeper into the binding pocket, the coplanar stacking of the benzamide ring and Phe121 is disrupted.

Discussion

Dopamine D-2 receptor model

A number of groups have developed theoretical models of GPCRs. Several different approaches described below have been taken. We have applied a combination of these approaches.

1. *Complete de novo design:* Baldwin [43, 44] used structural information extracted from a detailed analysis of the sequences. Another example of a computational approach can be found in Cronet et al. [48] Using the primary sequence of Rho Mirzadegan et al. [49] built a 3D structure for this G protein-coupled receptor. We use Baldwin's helical wheel approach to guide our modification of the relative helical orientation in our model.
2. *Some reliance on BRD structure:* Hutchins [32] modeled α-helices with ϕ/ψ=–55/–47, adjusted for proline and used BRD electron diffraction data to arrange the helices with respect to each other. Hibert et al., [50] and Trumpp-Kallmeyer [20] modeled α-helices with ϕ/ψ=–59/–44 and used BRD as a template for the relative positioning of the α-helical main axes. Other examples of this approach may be found in Dahl et al., [51], Grotzinger et al., [52] Ijzerman et al., [53] Lewell [7] and Mirzadegan and Liu.[49]
3. *Major reliance on BRD:* Teeter et al., [18] used BRD coordinates followed by modifications to the structure. Our initial modeling strategy was similar to this approach in that we used the bacteriorhodopsin data [34] to obtain an initial set of coordinates for the seven α-helices followed by adjustment for Pro bends. Our approach diverged from Teeter after this point because we then allowed considerable freedom in adjusting the rotation, translation and tilt of the helices.
4. *Modeling using the rhodopsin structure:* An example of the use of this G protein-coupled 9 Å low resolution crystal structure can be found in Jacobson et al. [54] We use the Rho projection map to help guide our adjustment of the relative orientation of the α-helices.

As demonstrated by Baldwin and others, the helical wheel representation is a useful tool for developing GPCR models. Helical wheels are used to illustrate the amphipathicity of the α-helices in GPCRs. That is the

hydrophobic residues are located outward toward the lipid membrane while the hydrophillic residues are located within the interior of the seven transmembrane domain. The amphipathic character of the α-helices is taken into account when adjusting the relative helical orientation. Figure 5 is the helical wheel of BRD and our model of D2 GPCR analogous to Baldwins figure five. [43] This illustrates the similarity between our and Baldwin's GPCR model. It also compares to Schertler's projection density maps of BRD and Rho which clearly demonstrate that BRD and Rho have different helical orientations. [38]

Discussion of docking results

Docking of the three different molecules were analyzed and compared primarily with those observed by Teeter [18] in the "binding pocket", which is described as the entire interior pocket of the receptor and encompasses three areas: the binding pocket where the agonists dock, the ancillary pocket where some antagonists may extend to, and the sodium binding site.

Dopamine docking

There are a number of aromatic residues (colored tan in Fig. 7) in the binding pocket midway into the transmembrane region (See Fig. 3 for our numbering of these residues). In particular, Phe121 and Trp155 closely (<2.5 Å) surround the phenyl of dopamine in an orthogonal orientation as seen in Fig. 7. There is another set of residues (colored blue) located in the lower part of the transmembrane region (closer to the cytoplasm) that Teeter [18] proposes is involved in the functioning of the Na+ channel (Fig. 4). We are studying these further to understand the possible implications better.

Our model shows almost all of the same binding pocket residues as Teeter. Close agreement between the models is expected since we followed essentially the same modeling approach (e.g., direct transfer of BRD coordinates to model the D-2 sequence for these docking studies). Teeter has a few residues within her binding pocket (Trp95/115, Phe159/186, our numbering/Teeters numbering) that did not move directly into our binding pocket upon docking. This difference may have resulted from differences in docking procedures. Further docking/comparison studies will be continued. The Trumpp-Kallmeyer [20] model shows a subset of our residues in her binding pocket for D-2. A closer examination of her model may identify additional similarities.

Site-specific mutagenesis experiments of D-2 receptors have demonstrated that primary interaction of dopamine occurs with aspartate-67 in the form of a salt bridge in the third transmembrane region of the dopamine receptors. [45, 55] Mutations of the aspartate-67 to asparagine or glycine eliminated the binding of both agonists and antagonists. The importance of serine residues in the fifth transmembrane region has also been investigated. [45, 56] Three conserved serine residues (116, 117 and 120) in the fifth transmembrane region have been shown to interact with the catechol moiety of dopamine. Serine-116 plays an important role in the binding of dopamine and the agonists. Mutation of serine-117 completely abolished the ability of dopamine to inhibit production of cAMP, whereas serine-116 and serine-120 mutations had much less effect.[56] The substituted benzamide, sulpiride, has been shown to exhibit a pH-dependence in the binding to D-2 receptors.[57] A histidine residue suspected to be within the ligand binding region from modeling studies may be involved in the pH-dependent binding of substituted benzamides. However, mutation of this histidine residue in the sixth transmembrane region to a leucine had only minor influence on the binding of a range of antagonists and did not change the pH-dependence of binding.[58]

Fallypride docking

The antagonist fallypride, a substituted benzamide, [26, 59] was docked in a manner similar to dopamine (Figs 9, 10). Constraints were applied between the ammonium nitrogen of fallypride and the helix3:Asp67 oxygens and between the fallypride methoxy OCH3's (oxygen) and helix5:Ser117,120 OH's (hydrogens). Constrained residues are colored red. Because fallypride was constrained to the two serines, it fits into the binding pocket in a similar fashion to dopamine. A third serine in helix 4 (helix4:Ser98) can hydrogen bond to the peptide carboxyl oxygen in fallypride. The Phe121 and Trp155 change their orientation about the fallypride phenyl ring and are not as close (~4 Å) as in the dopamine docking.

Our antagonist docking differs from Teeter because we are looking at a different class of compounds. Teeter docked tricyclic antagonists which lie parallel to the membrane plane. Dopamine and fallypride lie parallel to the helices. This can be seen clearly in a side-by-side comparison of dopamine and fallypride in Fig. 6.

In a related series of docking experiments the constraints between the methoxy OCH3's (oxygen) and helix5:Ser117,120 OH's (hydrogens) were eliminated leaving only one constraint between the ammonium nitrogen of fallypride and the helix3:Asp67 oxygens (Fig. 10).

We also docked the iso-butyl derivative of fallypride (Fig. 11) in an attempt to corroborate the results obtained by Mukherjee et al..[59] In this work it was found that although the iso-butyl derivative of fallypride had an apparent lipophilicity of k_w=2.5, its binding affinity was low due to possible steric hindrance. To enhance the possibility of a suitable docking of this ligand, we did not tether the molecule to the Ser117 and Ser120. We observed a substantial steric hindrance that could not be overcome. Basically, the presence of the iso-butyl group prevented the molecule from assuming the same docking orientation as fallypride because of steric hindrance of the iso-butyl group by His162 and Phe158. Removing

the tethering to Asp117 and 120 also did not improve the docking.

Comparison of dopamine and fallypride

We have previously shown that dopamine competes with fallypride. [28] This indicates a significant overlap of the binding of both dopamine and fallypride. This is evidenced from our docking results. We observed the requirement of an aspartate residue (Asp67) in helix-3 and the serine residues (serine-117 and serine-120) in helix-5 for both dopamine and fallypride. A significant interaction of the phenyl ring of fallypride was observed with Phe121 and Trp155, which was weaker in the case of dopamine. The *N*-allyl group of fallypride is flanked by Phe158 and His162, possibly enhancing pi-pi interaction. Furthermore, the fluoropropyl group in fallypride is flanked by helix5:Pro124, helix5:phe125 and helix3:Ile75 which seem to form a pocket. These additional interactions of fallypride give it a substantially higher affinity compared to that of dopamine.[28]

Conclusions

We have built a model of the D-2 dopaminergic receptor and docked the natural agonist dopamine and the dopamine derivative fallypride to the putative active site. Our modeling technique utilized information from several sources including 1. de novo structural data generated by modeling of helices based on the assignment of α-helix ϕ/ψ angles to the receptor primary sequence; 2. the results of helical wheel studies and techniques for rotational positioning of helices; 3. three dimensional structural information available for the BRD and Rho molecules for modeling by homology; 4. site-directed mutagenesis data for guidance in the placement of individual amino acids, and 5. structure-activity studies of specific lead compounds.

We believe the strength of our model is due to our efforts to integrate the available information and develop a systematic and balanced approach to utilize these data in the model building process. The chief impediment to accurate model construction is the lack of high resolution structural information by which to build by homology techniques. Subsequent modeling efforts will make use of additional information from any or all of the above sources as it becomes available.

In order to compare our model with previously published models, we docked the natural agonist dopamine. The results of this docking were similar to published work, suggesting that our model for D-2 was generally consistent in overall structure to that of others. Docking of fallypride provided an orientation that yielded several strong interactions. In the case of the D-2 model based on bacteriorhodopsin modified after consideration of structural information available from Rho, docking of fallypride provided a complex with several strong interactions. We would now like to dock derivative compounds in an attempt to help explain this phenomenon and shed light on their in vitro behavior. Additional antagonist mutation/binding data will be useful in helping to refine the antagonist-receptor complex.

Molecular modeling techniques hold great promise for the efficient design of selective and specific ligands. Improved computational techniques, faster computers and more accurate structural information integrated with the results of in vitro binding studies, site-directed mutagenesis work and in vivo observations will provide an increasingly fertile perspective for the design of useful drugs and improved understanding of their action at the molecular level. Ultimately, access to high resolution time-resolved structural data will provide definitive answers to the structure/function of the G-protein linked receptors.

Acknowledgments Supported in part by grants from the Department of Energy (DE-FG02–86-ER60437) and National Science Foundation (DBI-9730897) (to OHK), DE-FG02–94ER61840 (to JM) and DE-FG05–93-ER61588 (to RCR).

References

1. Bikker, J. A.; Trumpp-Kallmeyer, S.; Humblet, C. *J. Med. Chem*. **1998**, *41*, 2911.
2. Blundel, T. L.; Johnson, M. S.; Overington, J. P.; Sali, A. In *Protein design and the development of new therapeutics and vaccines*; Hook, J. B., Poste, G. T., Eds.; Plenum Press, NY, 1990; pp. 209–227.
3. Fong, T. M.; Strader, C. D. *Med. Res. Revs*. **1994**, *14*, 387.
4. Harrold, M. W.; Wallace, R. A.; Farooqi, T.; Wallace, L. J.; Uretsky, N.; Miller, D. D. *J. Med. Chem*. **1985**, *32*, 874.
5. Horstman, D. A.; Brandon, S.; Wilson, A. L.; Guyer, C. A.; Cragoe, E. J.; Limbird, L. *J. Biol. Chem*. **1990**, *265*, 21590.
6. Kapp, O. H.; Siemion, J.; Eckelman, W. C.; Cohen, V. I.; Reba, R. C. *Receptors and Signal Transduction*. **1997**, *7*, 177.
7. Lewell, X. Q. *Drug Design Discov*. **1992**, *9*, 29.
8. Pollock, N. J.; Manelli, A. M.; Hutchins, C. W.; Steffey, M. E.; MacKenzie, R. G.; Frail, D. E. *J. Biol. Chem*. **1992**, *267*, 17780.
9. Seeman, P.; Watanabe, M.; Grigoriadis, D.; Tedesco, J. L.; George, S.; Svensson, U.; Nilsson, J. L. G.; Neumeyer, J. L. *Mol. Pharmacol*. **1986**, *28*, 391.
10. Strader, C. D.; Sigal, I. S.; Register, R. B.; Candelore, M. R.; Rands, E.; Dixon, R. A. F. *Proc. Natl. Acad. Sci. USA*, **1987**, *84*, 4384.
11. Strader, C. D.; Sigal, I. S.; Candelore, M. R.; Rands, E.; Hill, W. S.; Dixon, R. A. F. *J. Biol. Chem*., **1988**, *263*, 10267.
12. Strader, C. D.; Candelore, M. R.; Hill, W. S.; Sigal, I. S.; Dixon, R. A. F. *J. Biol. Chem*. **1989**, *264*, 13572.
13. Strader, C. D.; Fong, T. M.; Tota, M. R.; Underwood, D.; Dixon, R. A. F. *Annu. Rev. Biochem*. **1994**, *63*, 101.
14. Strange, P. G. *Neurochem. Int*. **1993**, *22*, 223.
15. Summers, R. J.; McMartin, L. R. *J. Neurochem*. **1993**, *60*, 10.
16. Sunahara, R. K.; Seeman, P.; Van Tol, H. H. M.; Niznik, H. B. *Br. J. Psychiatry* **1993**, *163*(Suppl. 22), 31.
17. Suryanarayana, S.; Daunt, D. A.; von Zastrow, M.; Kobilka, B. K. *J. Biol. Chem*., **1991**, *266*, 15488.
18. Teeter, M. A.; Froimowitz, M.; Stec, B.; DuRand, C. J. *J. Med. Chem*. **1994**, *37*, 2874.
19. Tomic, M.; Seeman, P.; George, S. R.; O'Dowd, B. F. *Biochem. Biophys. Res. Commun*. **1993**, *191*, 1020.
20. Trumpp-Kallmeyer, S.; Bruinvels, A.; Hibert, M. *J. Med. Chem*. **1992**, *35*, 3448.

21. van Neuren, A. S.; Muller, G.; Klebe, G.; Moroder, L. *J. Recept Signal Transduct. Res*. **1999**, *19*, 341.
22. Verlet, L. *Phys. Rev*. **1967**, *159*, 98.
23. Wang, C. D.; Buck, M. A.; Fraser, C. M. **1991**, *40*, 168.
24. Wess, J. *Life Sci.* **1993**, *53*, 1447.
25. Civelli O.; Bunzow, J. R.; Grandy, D. K. *Ann. Rev. Pharmacol. Toxicol.* **1993**, *32*, 281.
26. Mukherjee, J.; Yang, Z. Y.; Brown, T.; Jiang, M.; Kapp, O. H.; Chen, C.-T.; Cooper, M. *Med. Chem. Res*. **1995**, *5*, 174.
27. Mukherjee, J.; Yang, Z. Y.; Brown, T.; Lew, R.; Wernick, M.; Ouyang, X.; Yasillo, N.; Chen, C.-T., Mintzer, R.; and Cooper, M. *Nucl. Med. Biol.*, **1999**, *26*, 519.
28. Mukherjee, J.; Yang, Z. Y.; Lew, R.; Brown, T.; Kronmal, S.; Cooper, M.; Seiden, L. S. *Synapse*, **1997**, *27*, 1.
29. Ballesteros, J. A.; Weinstein, H. *Methods Neurosci*. **1995**, *25*, 366.
30. Livingstone, C. D.; Strange, P. G.; Naylor, L. H. *Biochem. J*. **1992**, *287*, 277.
31. Livingstone, C. D.; Strange, P. G.; Naylor, L. H. *Biochem. Soc. Trans*. **1992**, *20*, 148S.
32. Hutchins, C. *Endocrine J*. **1994**, *2*, 7.
33. Probst, W. C.; Snyder, L. A.; Schuster, D. I.; Brosius, J.; Sealfon, S. C. *DNA Cell Biol*. **1992**, *11*, 1.
34. Henderson, R.; Schertler, G. F. X. *Phil. Trans. R. Soc. London* **1990**, *326*, 379.
35. Greer, J. *Proteins* **1990**, *7*, 317.
36. Needleman, S. B.; Wunsch, C. D. *J. Mol. Biol*. **1970**, *48*, 443.
37. Dayhoff, M. O.; Barker, W. C.; Hunt, L. T. *Methods Enzymol*. **1983**, *91*, 524.
38. Schertler, G. F. X.; Villa, C.; Henderson, R. *Nature* **1993**, *362*, 770.
39. Fine, R. M.; Wang, H.; Shenkin, P. S.; Yarmush, D. L.; Levinthal, C. *Proteins* **1986**, *1*, 342.
40. Dauber-Osguthorpe, P.; Roberts, V. A.; Osguthorpe, D. J.; Wolff, J.; Genest, M.; Hagler A. T. *Proteins Struct. Funct. Gene*. **1988**, *4*, 31.
41. Ponder, J. W.; Richards, F. M. *J. Mol. Biol*. **1987**, *193*, 775.
42. Mas, M. T.; Smith, K. C.; Yarmush, D. L.; Aisaka, K.; Fine, R. M. *Proteins Struct. Funct. Genet*. **1992**, *14*, 483.
43. Baldwin, J. M. *EMBO J*. **1993**, *12*, 1693.
44. Baldwin, J. M. *Curr. Opin. Cell Biol*. **1994**, *6*, 180.
45. Mansour, A.; Meng, F.; Meador-Woodruff, J. H.; Taylor, L. P.; Civelli, O.; Akil, H. *Eur. J. Pharmacol*. **1992**, *227*, 205.
46. Neve, K. A.; Cox, B. A.; Henningsen, R. A.; Spanoyannis, A.; Neve, R. L. *Mol. Pharmacol.* **1991**, *39*, 733.
47. Engelman, D. M.; Steitz, T. A. *Cell* **1981**, *23*, 411.
48. Cronet, P.; Sander, C.; Vried, G. *Prot. Eng*. **1993**, *6*, 59.
49. Mirzadegan, T.; Liu, R. S. H. *Prog, Retinal. Res*. 1992, *11*, 57.
50. Hibert, M. F.; Trumpp-Kallmeyer, S.; Bruinvels, A.; Hoflack, J. *Mol. Pharmacol*. **1991**, *40*, 8.
51. Dahl, S. G.; Edvardsen, O.; Sylte, I. *Proc. Natl. Acad. Sci. USA* **1991**, *88*, 8111.
52. Grotzinger, J.; Engles, M.; Jacoby, E.; Wollmer, A.; Strassburger, W. *Prot. Eng*. **1991**, *4*, 8.
53. Ijzerman, A. P.; Galen, P. J.; Jacobson, K. A. *Drug Design Discov*. **1992**, *9*, 49.
54. Jacobson, K. A.; Fischer, B.; van Rhee, A. M. *Life Sci.* **1995**, *56*, 49.
55. Neve, K. A. *Mol. Pharmacol.* **1991**, *39*, 570.
56. Cox, B. A.; Henningson, R. A.; Spanoyannis, A.; Neve, R. L.; Neve, K. A. *J. Neurochem*. **1992**, *59*, 627.
57. Presland, J. P.; Strange, P. G. *Biochem. Pharmacol*. **1991**, *41*, R9.
58. Woodward, R.; Daniell, S. J.; Strange, P. G.; Naylor, L. H. *J. Neurochem*. **1994**, *62*, 1664.
59. Mukherjee, J.; Yang, Z. Y.; Das, M. K.; Brown, T. *Nucl. Med. Biol.* **1995**, *22*, 283.
60. Dohlman, H. G.; Caron, M. G.; Strader, C. D. *Biochemistry* **1988**, *27*, 1813.
61. Chung, F.-Z.; Wang, C.-D.; Potter, P. C.; Venter, J. C.; Fraser, C. M. *J. Biol. Chem*. **1988**, *263*, 4052.
62. Dixon, R. A. F.; Sigal, I. S.; Candelore, M. R.; Register, R. B.; Scattergood, W.; Rands, E.; Strader, C. D. *EMBO J*. **1987**, *6*, 3269.
63. Kao, H.-T.; Adham, N.; Olsen, M. A.; Weinshank, R. L.; Brannchek, T. A.; Hartig, P. R. *FEBS Lett*., **1992**, *307*, 324.
64. Fraser, C. M.; Wang, C.-D.; Robinson, D. A.; Gocayne, J. D.; Venter, J. C. *Mol. Pharmacol*. **1989**, *36*, 840.
65. Kjelsberg, M. A.; Cotecchia, S.; Ostrowski, J.; Caron, M. G.; Lefkowitz, R. J. *J. Biol. Chem*. **1992**, *267*, 1430.
66. Choudhary, M. S.; Craigo, S.; Roth, B. L. *Mol. Pharmacol.* **1993**, *43*, 755.
67. Nakayama, T. A.; Khorana, H. G. *J. Biol. Chem*. **1991**, *266*, 4269.
68. Guan, X-M.; Peroutka, S. J.; Kobilka, B. K. *Mol. Pharmacol*. **1992**, *41*, 695.
69. Oksenberg, D.; Marsters, S. A.; O'Dowd, B. F.; Jin, H.; Havlik, S.; Peroutka, S. J.; Ashkenazi, A. *Nature* **1992**, *360*, 161.
70. Chanda, P. K.; Minchin, M. C. W.; Davis, A. R.; Greenberg, L.; Reilly, Y.; McGregor, W. H.; Bhat, R.; Iubeck, M. D.; Mizutani, S.; Hung, P. P. *Mol. Pharmacol.* **1993**, *43*, 111.